Received 7 February 2022; revised 13 March 2022; accepted 28 March 2022. Date of publication 5 April 2022; date of current version 19 April 2022.

Digital Object Identifier 10.1109/OJCOMS.2022.3164876

Performance Analysis of Uplink NOMA With Constellation–Rotated STLC for IoT Networks

KI-HUN LEE [1] (Student Member, IEEE), JEONG SEON YEOM [1] (Student Member, IEEE), JINGON JOUNG [2] (Senior Member, IEEE), AND BANG CHUL JUNG [1] (Senior Member, IEEE)

[1]Department of Electronics Engineering, Chungnam National University, Daejeon 34134, South Korea

[2]School of Electrical and Electronics Engineering, Chung-Ang University, Seoul 06974, South Korea

CORRESPONDING AUTHOR: B. C. JUNG (e-mail: bcjung@cnu.ac.kr)

This work was supported by the National Research Foundation of Korea (NRF) grant funded by the Korea Government (MSIT) under Grant NRF-2021R1A4A1032580.

ABSTRACT We investigate the uplink non-orthogonal multiple access (NOMA)-based Internet-of-Things (IoT) networks, where each IoT device (station: STA) equipped with a single antenna exploits the *constellation-rotated* space-time line code (CR-STLC) to send signals to an access point (AP) equipped with two receive antennas. The AP decodes the signals transmitted from the STAs with the *optimal* joint maximum-likelihood (JML) detector. As a main result, we mathematically analyze both the bit-error-rate (BER) performance and the spatial diversity order of each STA in the two-user uplink CR-STLC NOMA system. In particular, it is shown that the two-user uplink CR-STLC NOMA system achieves the optimal diversity order regardless of the constellation rotation angle in the high signal-to-noise ratio (SNR) regime. We also consider two different rotation angle optimization techniques (dynamic rotation & fixed rotation) to improve the BER performance in the practical SNR regime, and found that the fixed rotation approach is simple but yields almost the same performance as the dynamic approach. Finally, we show that the uplink CR-STLC NOMA system achieves the spatial diversity order of 1 even when more than two STAs send packets simultaneously. It is worth noting that all STAs obtain an improved spatial diversity gain compared to that without constellation rotation.

INDEX TERMS Bit-error-rate, constellation rotation, Internet-of-Things, joint maximum-likelihood detection, non-orthogonal multiple access, space-time line codes, spatial diversity, uplink networks.

I. INTRODUCTION

WITH the proliferation of wireless devices to realize hyper-connectivity networks including humans and Internet-of-Things (IoT), the sixth-generation (6G) networks are expected to require much higher spectral efficiency (SE), massive connectivity, energy efficiency (EE), and lower latency performance than the fifth-generation (5G) [1], [2]. To fulfill these requirements, non-orthogonal multiple access (NOMA) is being actively studied in both academia and industry as one of the most promising techniques for massive IoT networks [3]–[5]. Basically, the NOMA allows multiple devices to share the common radio resource blocks through power- or code-domain multiplexing, which are referred to as PD-NOMA and CD-NOMA, respectively. Thus, the NOMA can overcome the limitation of orthogonal multiple access (OMA)-based communication schemes such as limited radio resources, and significantly improve SE, EE, and system capacity [5]–[7].

In particular, since explosive traffic is expected in the uplink rather than the downlink in massive IoT networks, various techniques for NOMA-based uplink IoT networks are being studied recently. Introducing some of them, a single carrier index modulation-based NOMA technique for improving the EE of IoT devices and a signal detection technique considering the sporadic traffic patterns of IoT devices have been proposed in [8] and [9], respectively. Most existing studies on the uplink NOMA assume that channel state information (CSI) is known at the access point (AP), i.e., the

receiver (CSIR). However, in massive IoT networks, it seems infeasible for an AP to obtain full CSI from a massive number of IoT devices (stations: STAs) to itself due to significant signaling overhead [10], [11]. Instead, each STA can easily obtain its CSI from itself to the AP by observing the downlink common pilot signal broadcast from the AP, considering the channel reciprocity property in the time-division duplex (TDD) system [3], [12], which is a dominant frame structure of contemporary commercial wireless systems including the third generation partnership project (3GPP) 5G new radio (NR) [13], [14]. This motivates us to investigate the uplink NOMA system where CSI is known only at the transmitter (CSIT) in this paper.

With this perspective, the space-time line code (STLC)-based NOMA system (*STLC NOMA*) has been proposed for two-user uplink IoT networks, assuming that each STA has its own CSI, while the AP has only the channel gain of the wireless channel vector from each STA to itself, not full CSI of the STA (CSIT) in [15], [16]. The STLC was proposed in [17] as the symmetric communication technique of the well-known space-time block code (STBC). It is known that the STLC achieves full-rate and full-spatial diversity performance in the 1×2 single-input multiple-output (SIMO) systems when CSI is known to not the receiver but the transmitter. With a basic property of the STLC, the signals do not experience phase distortion like the conventional maximum ratio transmission (MRT) and the STLC receiver can blindly decode the received signals without CSI [18]. Furthermore, it can be implemented with a low-complexity linear encoding and decoding procedure [19], [20]. Through computer simulations in [15], [16], it was shown that the uplink STLC NOMA system achieves almost the same bit-error-rate (BER) performance as the OMA technique as signal-to-noise ratio (SNR) increases by applying the *constellation rotation* method to the STLC (we define this as constellation rotated (CR)-STLC).

The constellation rotation has been applied to the PD-NOMA systems for improving error performance or increasing sum-rate [21]–[25]. In particular, uplink NOMA systems require more sophisticated constellation rotation techniques than downlink because each user experiences independent fading channels with different phase distortions. In the downlink NOMA system, each STA receives superposed signals from the AP through its own channel, and the error performance can be improved by increasing Euclidean distances among constellation points [21], [22]. In the uplink, on the other hand, the AP receives the superimposed signals from multiple STAs where multiple signals from STAs experience different fading channels and the constellation phase of signal from each STA needs to be carefully adjusted at each STA before uplink signal transmission.

For this reason, in [23], it is assumed that an uplink user knows global CSI and even power ratio between its own signal and another user's signal. Based on this assumption, an instantaneous constellation rotation method was proposed for uplink SIMO NOMA systems. In [24],

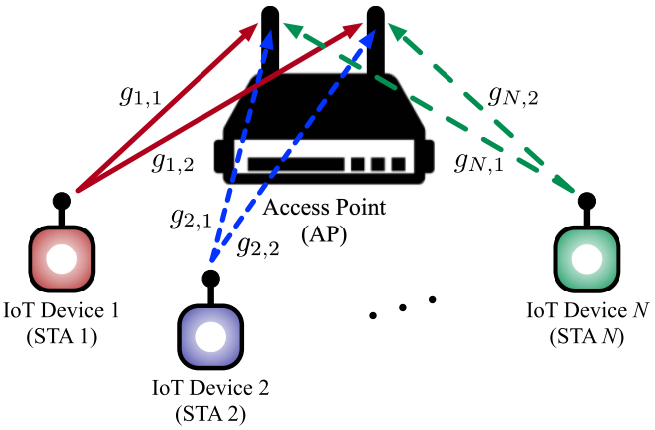

FIGURE 1. A system model of the NOMA-based uplink IoT network.

the constellation rotation technique was also proposed for an uplink single-input single-output (SISO) NOMA system under the assumption that multiple transmitters and a receiver have global CSI and the channel coefficients from multiple transmitters to a single receiver are controlled to be identical to each other. However, these assumptions may not be feasible due to the signaling overhead or power limitations at STAs in practical massive IoT networks. The constellation rotation was designed for increasing the constellation-constrained capacity in [24] and [25], not considering the error performance. Furthermore, existing studies adopted the successive interference cancellation (SIC) to detect multiple signals from STAs even though it does not result in an optimal performance in the uplink NOMA system, which has been known to have the error floor phenomenon. Recently, it has been shown that the joint maximum likelihood (JML) detector achieves the optimal performance with tolerable computational complexity in uplink NOMA systems [26]–[28].

Meanwhile, the error performance analysis of the NOMA system is being actively studied as summarized in [27], [29]. In particular, two-user and quadrature phase-shift keying (QPSK) modulation have been mainly investigated for uplink NOMA systems [26], [27]. In [30], the error rates have been analyzed for downlink/uplink NOMA systems that consider multi-user, 4-quadrature amplitude modulation (QAM), and the SIC receiver. Recently, generalized BER performance considering an arbitrary number of STAs, general modulation orders, and an arbitrary number of AP antennas has been mathematically analyzed for uplink and downlink in [28] and [29], respectively. However, these studies assume CSIR. In addition, the additive white Gaussian noise (AWGN) channel is considered and the fading effects due to wireless channels were not investigated in [27], [30]. It is worth noting that the uplink CR-STLC NOMA system considered in this paper is similar to [27] because the phase distortion caused by channels is compensated by STLC operations.

In this paper, we consider more than two IoT devices while only two IoT devices are considered in [15] and we provide novel theoretical results. Specifically, main contributions of this paper are summarized as follows.

- To the best of our knowledge, there is no study on the uplink NOMA system with CSIT except for our previous studies [15], [16]. We exploit the constellation rotation technique to improve performance in terms of BER rather than sum-rate. Unlike conventional constellation rotation methods applied to uplink NOMA systems, the proposed technique (especially the fixed rotation technique) does not require instantaneous CSI feedback or channel tuning.
- We mathematically analyze the BER performance of the CR-STLC NOMA system for two-user uplink IoT networks and it is validated through Monte-Carlo computer simulations.
- We consider both dynamic and fixed constellation rotation methods for the two-user uplink CR-STLC NOMA system, and then derive the optimal rotation-angle for a given SNR value to improve the BER performance in the practical SNR regime.
- We extend the system model of the uplink CR-STLC NOMA to the case where more than two STAs exist for massive IoT networks and mathematically analyze the spatial diversity order of each STA.

The remainder of this paper is organized as follows. In Section II, we introduce the system model of the CR-STLC NOMA system considering an uplink IoT network. In Section III, we mathematically analyze the BER performance and spatial diversity order for each STA. In Section IV, we derive the optimal rotation angle for the two-user uplink CR-STLC NOMA based on the minimum distance between constellation points and the average BER performance criteria, respectively. In Section V, we verify the analysis results by comparing them with computer simulations, and show various simulation results considering multiple STAs or other modulation schemes. Conclusion is drawn in Section VI.

Notations: Throughout this paper, $(\cdot)^*$, $|\cdot|$, and $\|\cdot\|$ denote the complex conjugate operator, the absolute value, and the Euclidean norm, respectively. If $|\cdot|$ is applied for a set, then it denotes the cardinality of the set, which is defined as the number of elements in the set. The term $\Pr(\cdot)$ denotes the probability of an event, $\mathbb{E}[\cdot]$ denotes the statistical expectation. Both $\Re[\cdot]$ and $\Im[\cdot]$ denote the real and imaginary components of a complex number, respectively. Moreover, $\lfloor\cdot\rfloor$ and $\lceil\cdot\rceil$ represent the floor function that gives the greatest integer number less than or equal to the input real number and the ceiling function that gives the least integer greater than or equal to the input real number, respectively. The vector or matrix transpose operation is denoted by $[\cdot]^{\mathrm{T}}$, the 2×2 identity matrix is denoted as $\mathbf{I}_2$, the imaginary unit is denoted by j, i.e., $j \triangleq \sqrt{-1}$, and the complex Gaussian random variable with a zero mean and σ^2 variance is denoted as $\mathcal{CN}(0,\sigma^2)$.

II. SYSTEM MODEL

We consider a NOMA-based uplink IoT network, in which N IoT devices (stations: STAs) equipped with a single antenna transmit data to an access point (AP) with two antennas, as illustrated in Fig. 1. The STAs obtain the CSI between themselves and the AP by overhearing the broadcast downlink common reference signals from the AP with the channel reciprocity property of TDD wireless communication systems [12]. It is assumed that the CSI is available only at each STA (CSIT) and the channel estimation is perfect. It is also assumed that each STA employs a quadrature phase-shift keying (QPSK) modulator for energy efficiency and low complexity of IoT networks. Each STA encodes two consecutive QPSK modulated symbols into two STLC signals exploiting its local CSI. Here, we apply *constellation-rotated STLC* (CR-STLC). The basic idea is to rotate the constellation of the QPSK symbol to a certain angle before STLC encoding to increase the minimum distance between the constellation points of the superimposed symbols, which dominantly affects the symbol- or bit-error. Specifically, each STA receives rotation angle $\theta_n[^\circ]$ ($n \in \{1,2,\ldots,N\}$, $0^\circ \le \theta_n < 45^\circ$) from the AP and then rotates the QPSK symbols to θ_n. Therefore, the CR-STLC signals of the nth STA to be transmitted at the time-slot t ($\in\{1,2\}$), $s_{n,t}$, are encoded as follows:

$$s_{n,1} = \sqrt{P_n}\frac{h_{n,1}^* x_{n,1} e^{j\theta_n} + h_{n,2}^* \left(x_{n,2} e^{j\theta_n}\right)^*}{\sqrt{|h_{n,1}|^2 + |h_{n,2}|^2}}, \qquad \text{for } t=1,$$
$$s_{n,2} = \sqrt{P_n}\frac{h_{n,2}^* \left(x_{n,1} e^{j\theta_n}\right)^* - h_{n,1}^* x_{n,2} e^{j\theta_n}}{\sqrt{|h_{n,1}|^2 + |h_{n,2}|^2}}, \qquad \text{for } t=2, \quad (1)$$

where $x_{n,t}$ denotes the normalized QPSK symbol of the nth STA at the time-slot t, such that $\mathbb{E}[|x_{n,t}|^2] = 1$, $\forall n,t$, and $h_{n,m}$ denotes the wireless channel coefficient between the nth STA and the m ($\in\{1,2\}$)th receive antenna of the AP. All wireless channels are assumed to follow identically and independently distributed (i.i.d.) complex Gaussian distribution with a zero mean and a unit variance, i.e., $h_{n,m} \sim \mathcal{CN}(0,1)$, $\forall n,m$, and to be static for at least *two* time-slots.[1] Also, P_n is the fixed average transmit power of the nth STA depending on the energy status of STAs and the channel conditions, such that $\mathbb{E}[\|\mathbf{s}_n\|^2] = 2P_n$, where $\mathbf{s}_n = [s_{n,1}\ s_{n,2}]^{\mathrm{T}}$.

The STAs transmit CR-STLC signals to the AP simultaneously during two time-slots through the common radio resource block. The received signals at two antennas of the

1. The 5G NR supports flexible transmission time interval (TTI) according to the numerology with TDD operation. The downlink and uplink transmissions can also be dynamically switched in each TTI. In general, the time duration of the TTI is determined so that it is smaller than a channel coherence time and the channel reciprocity property between downlink and uplink are preserved [12], [13]. This is more reasonable for IoT networks since most IoT applications request to send short packets and most IoT devices are fixed over time [31].This implies that the wireless channels can be assumed to be static within each TTI in practice. For our system model, we can regard the two consecutive time-slots consisting of downlink and uplink as a single TTI in 5G NR systems.

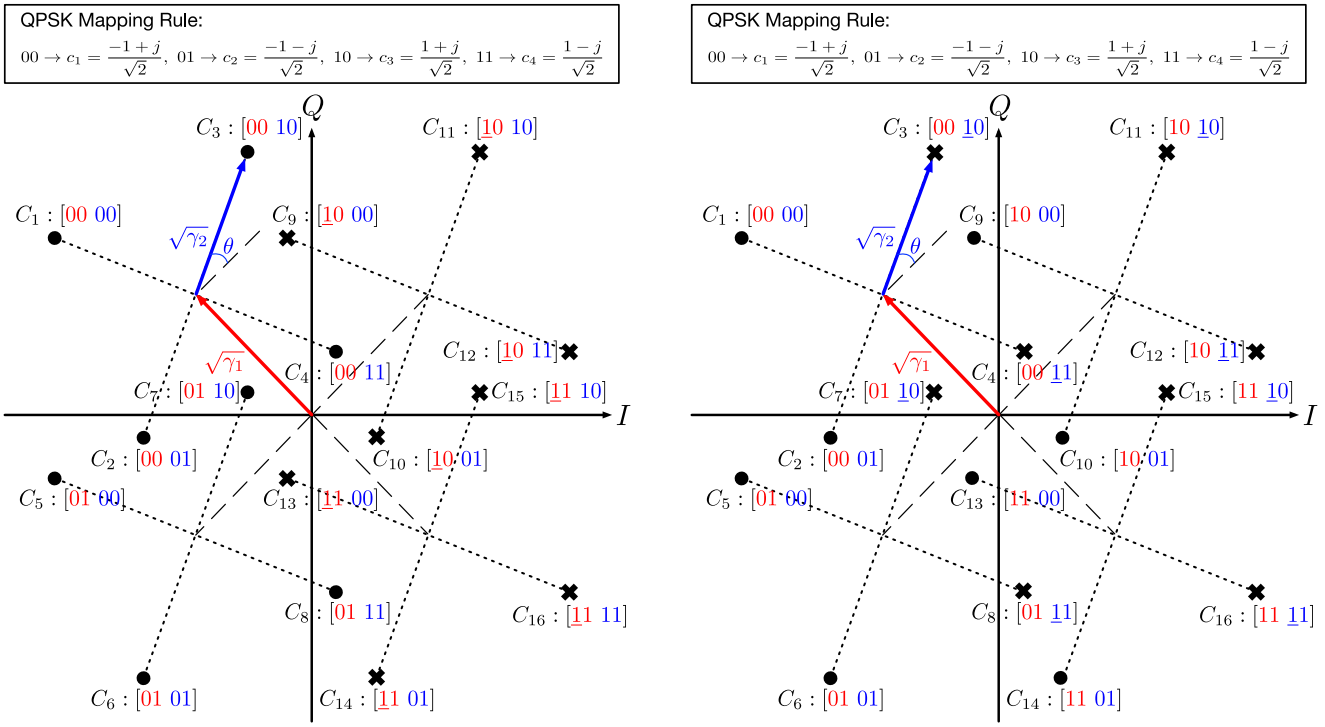

(a) First STA (b) Second STA

FIGURE 2. Received signal constellation of superimposed QPSK symbols in the two-user uplink CR-STLC NOMA and error event, when $P_1\gamma_1 = P_2\gamma_2$.

AP are then written as:

$$y_{m,t} = \sum_{n=1}^{N} \sqrt{d_n^{-\alpha}} h_{n,m} s_{n,t} + w_{m,t}, \quad \forall m, t, \tag{2}$$

where $y_{m,t}$ denotes the received signal of the mth antenna at the time-slot t, and $w_{m,t} \sim \mathcal{CN}(0, N_0)$ denotes the additive white Gaussian noise at the $y_{m,t}$. Also, d_n and α denote the distance from the nth STA to the AP and the path-loss exponent, respectively.

From (2), the AP performs STLC decoding [17] that is a simple linear combining procedure as follows:

$$\begin{aligned} r_1 &= y_{1,1} + y_{2,2}^* = \sum_{n=1}^{N} \sqrt{P_n d_n^{-\alpha}} \|\mathbf{h}_n\| x_{n,1} e^{j\theta_n} + w_{1,1} + w_{2,2}^*, \\ r_2 &= y_{2,1}^* - y_{1,2} = \sum_{n=1}^{N} \sqrt{P_n d_n^{-\alpha}} \|\mathbf{h}_n\| x_{n,2} e^{j\theta_n} + w_{2,1}^* - w_{1,2}, \end{aligned} \tag{3}$$

where r_t represents the tth STLC decoding signal and $\mathbf{h}_n$ $(= [h_{n,1}\ h_{n,2}]^{\mathrm{T}})$ denotes the channel coefficient vector from the nth STA to the AP. We can observe that each r_t has the ordinary QPSK symbols of N STAs corresponding to the time-slot t without phase distortion by wireless channels. Note that the signals are still rotated to θ_n as predefined, and the variance of the noise is doubled to $2N_0$.

The AP then detects the QPSK symbols of each STA, $x_{n,t}$ for all n and t, through the JML detector considering the rotation angles. Let γ_n be the effective channel gain of the nth STA defined as $\gamma_n \triangleq \|\mathbf{g}_n\|^2$, where $\mathbf{g}_n \triangleq \sqrt{d_n^{-\alpha}}\mathbf{h}_n$, i.e., $\mathbf{g}_n \sim \mathcal{CN}(\mathbf{0}, d_n^{-\alpha} \cdot \mathbf{I}_2)$. It is assumed that the AP knows the partial CSI, which is the effective channel gain of each STA by using the *blind energy estimation method* based on the clustering algorithm such as k-means and Gaussian mixture model without the pilot signal [32]–[34]. For example, a soft k-means clustering method (expectation-maximization (EM) algorithm) can be exploited to blindly estimate the channel gains of multiple STAs in uplink CR-STLC NOMA systems, which infers the means of the Gaussian mixture model for given the number of STAs and modulation orders. Of course, there may exist estimation errors in practice, but in this paper, we assume that the AP perfectly estimates the effective channel gain of each STA. It is worth noting that the results derived under this assumption is still meaningful in that it can represent an upper bound on the fundamental performance of the uplink CR-STLC NOMA system. Then, the estimate of all signals are represented as follows:

$$[\widehat{x}_{1,t}, \ldots, \widehat{x}_{N,t}] = \arg \min_{x_{n,t} \in \mathcal{X}} \left| r_t - \sum_{n=1}^{N} \sqrt{P_n}\sqrt{\gamma_n} x_{n,t} e^{j\theta_n} \right|^2,$$

where $\mathcal{X}$ is a set of normalized QPSK symbols, i.e., $\mathcal{X} \triangleq \{c_1, c_2, c_3, c_4\} = \{\frac{-1+j}{\sqrt{2}}, \frac{-1-j}{\sqrt{2}}, \frac{1+j}{\sqrt{2}}, \frac{1-j}{\sqrt{2}}\}$.

III. PERFORMANCE ANALYSIS

In this section, we mathematically analyze the BER performance and the spatial diversity order of each STA

TABLE 1. Euclidean distances set 1 ($\mu = \cos\theta + \sin\theta$ and $\nu = \cos\theta - \sin\theta$).

p	$\{\alpha_{p,q}, \beta_{p,q}, \zeta_{p,q}\}$							
	$q=9$	$q=10$	$q=11$	$q=12$	$q=13$	$q=14$	$q=15$	$q=16$
1	$2,0,0$	$2,2,4\sin\theta$	$2,2,4\cos\theta$	$2,4,4\mu$	$4,0,0$	$4,2,4\mu$	$4,2,4\nu$	$4,4,8\cos\theta$
2	$2,2,-4\sin\theta$	$2,0,0$	$2,4,4\nu$	$2,2,4\cos\theta$	$4,2,-4\mu$	$4,0,0$	$4,4,-8\sin\theta$	$4,2,4\nu$
3	$2,2,-4\cos\theta$	$2,4,-4\nu$	$2,0,0$	$2,2,4\sin\theta$	$4,2,-4\nu$	$4,4,8\sin\theta$	$4,0,0$	$4,2,4\mu$
4	$2,4,-4\mu$	$2,2,-4\cos\theta$	$2,2,-4\sin\theta$	$2,0,0$	$4,4,-8\cos\theta$	$4,2,-4\nu$	$4,2,-4\mu$	$4,0,0$
5	$4,0,0$	$4,2,-4\nu$	$4,2,4\mu$	$4,4,8\sin\theta$	$2,0,0$	$2,2,4\sin\theta$	$2,2,4\cos\theta$	$2,4,4\mu$
6	$4,2,4\nu$	$4,0,0$	$4,4,8\cos\theta$	$4,2,4\mu$	$2,2,-4\sin\theta$	$2,0,0$	$2,4,4\nu$	$2,2,4\cos\theta$
7	$4,2,-4\mu$	$4,4,-8\cos\theta$	$4,0,0$	$4,2,-4\nu$	$2,2,-4\cos\theta$	$2,4,-4\nu$	$2,0,0$	$2,2,4\sin\theta$
8	$4,4,-8\sin\theta$	$4,2,-4\mu$	$4,2,4\nu$	$4,0,0$	$2,4,-4\mu$	$2,2,-4\cos\theta$	$2,2,-4\sin\theta$	$2,0,0$

in the uplink CR-STLC NOMA system. Specifically, before Section III-D, we first consider the two-user uplink NOMA system, i.e., $N = 2$, which has been strikingly investigated in many literature [8], [9], [15], [16], [23]–[27]. Then, the spatial diversity order analysis for the uplink CR-STLC NOMA system is derived for more than two STAs ($N \geq 3$) in Section III-D.

A. BER OF THE FIRST STA

In the two-user uplink CR-STLC NOMA systems, since the angle difference between θ_1 and θ_2, $|\theta_1 - \theta_2|$, is critical for BER, without loss of generality (w.l.o.g.), only the QPSK symbols of the second STA for two time-slots are assumed to be rotated by θ, i.e., $\theta_1 = 0$ and $\theta_2 = \theta$. Fig. 2 shows the superimposed QPSK symbols, r_t ($t \in \{1, 2\}$), which are the decoded signals from the received CR-STLC signals at the AP. In addition, this figure shows the QPSK mapping rule of each point, and $C_i = \sqrt{P_1\gamma_1}c_{\lceil i/4\rceil} + \sqrt{P_2\gamma_2}e^{j\theta}c_{(((i-1)\bmod 4)+1)}$ ($i \in \{1, 2, \ldots, 16\}$), in which the first and last two bits are for STA 1 and 2, respectively. We only consider, w.l.o.g., error cases where the *first* bit of the *first* STA for time-slot 1 is zero to one due to the symmetry.[2] Therefore, the bit error event occurs at the AP when the JML detector detects one of the '×' marks not '•' marks for the first STA as shown in Fig. 2(a).

By exploiting the union bound technique of the detection error probability, the conditional BER of the first STA for given channel gains, namely γ_1 and γ_2, is derived as follows:

$$\begin{aligned}&\Pr(\mathcal{E} \mid \gamma_1, \gamma_2, \theta, b_{1,1} = 0)\\ &\leq \sum_{p=1}^{8}\sum_{q=9}^{16}\Pr\big(C_p \mid b_{1,1} = 0\big)\Pr\big(C_q \mid \gamma_1, \gamma_2, \theta, C_p\big)\\ &\overset{(a)}{\leq} \sum_{p=1}^{8}\sum_{q=9}^{16}\frac{1}{8}Q\left(\sqrt{\frac{\delta_{p,q}^2}{4N_0}}\right),\end{aligned} \tag{4}$$

2. Since the signals for each time-slot of both STAs are independently detected from each STLC decoding signal (3) through the JML detector and the two signals form the same constellation, the BER for each time-slot is the same. Considering the error event of the first STA, the error performances of the two bits in a QPSK symbol are the same to each other as well. By the symmetry of QPSK modulation, the conditional bit error probabilities are the same when 0 and 1 are assumed to be sent.

where $\mathcal{E}$ denotes the bit-error event for given conditions, $b_{n,l}$ ($n \in \{1, 2\}, l \in \{1, 2\}$) denotes the lth bit of the STA n, $\delta_{p,q}$ denotes the Euclidean distance between the constellation points C_p ($p \in \{1, 2, \ldots, 8\}$), i.e., *bit-correct point*, and C_q ($q \in \{9, 10, \ldots, 16\}$), i.e., *bit-error point*. Since the probabilities that each QPSK symbol is transmitted are equal, i.e., $\Pr(C_p \mid b_{1,1} = 0) = 1/8$, (a) is satisfied. We then derive a general detection error probability for all pairs of bit-correct point and bit-error point.

Considering the transmit symbols of both STAs and the rotation angle, the general Euclidean distance is derived as

$$\delta_{p,q} = \sqrt{\alpha_{p,q}P_1\gamma_1 + \beta_{p,q}P_2\gamma_2 + \zeta_{p,q}\sqrt{P_1P_2}\sqrt{\gamma_1\gamma_2}}, \tag{5}$$

where $\alpha_{p,q}$, $\beta_{p,q}$, and $\zeta_{p,q}$ are given in Table 1 for all p and q. Here, $\mu = \cos\theta + \sin\theta$ and $\nu = \cos\theta - \sin\theta$. Note that $\zeta_{p,q}$ is a function related on θ.

For the tractable analysis of the BER performance, we use an upper bound of the Q-function in [35], the *exponential bound* defined as

$$Q\left(\sqrt{\frac{\delta_{p,q}^2}{4N_0}}\right) \leq \frac{1}{2}\sum_{v=1}^{V}a_v\exp\left(-b_v\frac{\delta_{p,q}^2}{8N_0}\right), \tag{6}$$

where $a_v = 2(\lambda_v - \lambda_{v-1})/\pi$; $b_v = 1/\sin^2\lambda_v$; $\lambda_v = v\pi/2V$ for $v = 1, 2, \ldots, V$; and $\lambda_0 = 0$. As V increases, the tighter exponential bound (6) is achieved ($V = 50$ is sufficient for the tight bound as shown in Section V).

From (4) to (6), the upper bound expression of the BER performance of the *first* STA in the two-user uplink CR-STLC NOMA system, denoted by $P_{b,1}$, can be derived as follows:

$$\begin{aligned}P_{b,1} &\leq \frac{1}{8}\sum_{p=1}^{8}\sum_{q=9}^{16}\mathbb{E}_{Z_1,Z_2}\left[\frac{1}{2}\sum_{v=1}^{V}a_v\exp\left(-b_v\frac{\delta_{p,q}^2}{8N_0}\right)\right]\\ &= \frac{1}{16}\sum_{p=1}^{8}\sum_{q=9}^{16}\sum_{v=1}^{V}a_v\mathbb{E}_{Z_1,Z_2}\left[\exp\left(-b_v\frac{\delta_{p,q}^2}{8N_0}\right)\right],\end{aligned} \tag{7}$$

where random variables are defined as $Z_n := \gamma_n$, $\forall n$ for channel gains.

Let's define $\sigma_n \triangleq d_n^{-\alpha}$ for simplicity. Then, the probability density function (PDF) of Z_n is given by $f_{Z_n}(z_n) =$

TABLE 2. Euclidean distances set 2 ($\mu = \cos\theta + \sin\theta$ and $\nu = \cos\theta - \sin\theta$).

p	$\{\alpha_{p,q}, \beta_{p,q}, \zeta_{p,q}\}$							
	$q=3$	$q=4$	$q=7$	$q=8$	$q=11$	$q=12$	$q=15$	$q=16$
1	$0,2,0$	$0,4,0$	$2,2,-4\sin\theta$	$2,4,4\nu$	$2,2,4\cos\theta$	$2,4,4\mu$	$4,2,4\nu$	$4,4,8\cos\theta$
2	$0,4,0$	$0,2,0$	$2,4,-4\mu$	$2,2,-4\sin\theta$	$2,4,4\nu$	$2,2,4\cos\theta$	$4,4,-8\sin\theta$	$4,2,4\nu$
5	$2,2,4\sin\theta$	$2,4,-4\nu$	$0,2,0$	$0,4,0$	$4,2,4\mu$	$4,4,8\sin\theta$	$2,2,4\cos\theta$	$2,4,4\mu$
6	$2,4,4\mu$	$2,2,4\sin\theta$	$0,4,0$	$0,2,0$	$4,4,8\cos\theta$	$4,2,4\mu$	$2,4,4\nu$	$2,2,4\cos\theta$
9	$2,2,-4\cos\theta$	$2,4,-4\mu$	$4,2,-4\mu$	$4,4,-8\sin\theta$	$0,2,0$	$0,4,0$	$2,2,-4\sin\theta$	$2,4,4\nu$
10	$2,4,-4\nu$	$2,2,-4\cos\theta$	$4,4,-8\cos\theta$	$4,2,-4\mu$	$0,4,0$	$0,2,0$	$2,4,-4\mu$	$2,2,-4\sin\theta$
13	$4,2,-4\nu$	$4,4,-8\cos\theta$	$2,2,-4\cos\theta$	$2,4,-4\mu$	$2,2,4\sin\theta$	$2,4,-4\nu$	$0,2,0$	$0,4,0$
14	$4,4,8\sin\theta$	$4,2,-4\nu$	$2,4,-4\nu$	$2,2,-4\cos\theta$	$2,4,4\mu$	$2,2,4\sin\theta$	$0,4,0$	$0,2,0$

$(z_n/\sigma_n^2)\exp(-z_n/\sigma_n)$ from the definition of γ_n. The expectation term in (7) can be derived as follows:

$$\begin{aligned}
&\mathbb{E}_{Z_1,Z_2}\left[\exp\left(-b_v\frac{\delta_{p,q}^2}{8N_0}\right)\right]\\
&=\int_0^\infty\int_0^\infty \exp\left(-b_v\frac{\delta_{p,q}^2}{8N_0}\right)f_{Z_1}(z_1)f_{Z_2}(z_2)dz_1dz_2\\
&=\int_0^\infty\int_0^\infty \exp\left(-b_v\frac{\alpha_{p,q}P_1z_1+\beta_{p,q}P_2z_2+\zeta_{p,q}\sqrt{P_1P_2}\sqrt{z_1z_2}}{8N_0}\right)\\
&\quad\times\frac{z_1}{\sigma_1^2}\exp\left(-\frac{z_1}{\sigma_1}\right)\frac{z_2}{\sigma_2^2}\exp\left(-\frac{z_2}{\sigma_2}\right)dz_1dz_2\\
&=\frac{1}{\sigma_1^2\sigma_2^2}\Bigg[\frac{1}{A^2}+\frac{\rho_1\rho_2}{2^7}\frac{b_v^2\zeta_{p,q}^2}{A^3}+\frac{15\rho_1\rho_2}{2^4}\frac{b_v^2\zeta_{p,q}^2}{B^3}\\
&\quad+\frac{3\rho_1^2\rho_2^2}{2^{10}}\frac{b_v^4\zeta_{p,q}^4}{AB^3}-\frac{5\rho_1^3\rho_2^3}{2^{18}}\frac{b_v^6\zeta_{p,q}^6}{A^2B^3}+\frac{\rho_1^4\rho_2^4}{2^{25}}\frac{b_v^8\zeta_{p,q}^8}{A^3B^3}\\
&\quad-\left(\frac{9\sqrt{\rho_1\rho_2}}{2}\frac{b_v\zeta_{p,q}}{B^{5/2}}+\frac{15\sqrt{\rho_1\rho_2}^3}{2^7}\frac{b_v^3\zeta_{p,q}^3}{B^{7/2}}\right)\Phi\big(b_v,\zeta_{p,q},B\big)\Bigg],
\end{aligned}\tag{8}$$

where $\rho_n = P_n/N_0$ denotes the system SNR of the nth STA,

$$\Phi\big(b_v,\zeta_{p,q},B\big)=\begin{cases}\tan^{-1}\left(\frac{8}{\sqrt{\rho_1\rho_2}b_v\zeta_{p,q}}\sqrt{B}\right), & \text{if } \zeta_{p,q}\geq 0,\\ \pi-\tan^{-1}\left(\frac{8}{\sqrt{\rho_1\rho_2}b_v\zeta_{p,q}}\sqrt{B}\right), & \text{if } \zeta_{p,q}<0,\end{cases}$$

and

$$A=\frac{\alpha_{p,q}\beta_{p,q}}{64}\rho_1\rho_2b_v^2+\frac{\sigma_1\alpha_{p,q}\rho_1+\sigma_2\beta_{p,q}\rho_2}{8\sigma_1\sigma_2}b_v+\frac{1}{\sigma_1\sigma_2},$$
$$B=\frac{4\alpha_{p,q}\beta_{p,q}-\zeta_{p,q}^2}{64}\rho_1\rho_2b_v^2+\frac{\sigma_1\alpha_{p,q}\rho_1+\sigma_2\beta_{p,q}\rho_2}{2\sigma_1\sigma_2}+\frac{4}{\sigma_1\sigma_2}.$$

By substituting (8) to (7), the closed-form of the BER upper bound of the first STA is achieved.

B. BER OF THE SECOND STA

With the same approach as Section III-A, from (7), the BER upper bound of the *second* STA in the two-user uplink CR-STLC NOMA system, $P_{b,2}$, can be derived as follows:

$$P_{b,2}\leq\frac{1}{16}\sum_{p\in\mathcal{P}}\sum_{q\in\mathcal{Q}}\sum_{v=1}^{V}a_v\mathbb{E}_{Z_1,Z_2}\left[\exp\left(-b_v\frac{\delta_{p,q}^2}{8N_0}\right)\right],\tag{9}$$

where $\mathcal{P}=\{1,2,5,6,9,10,13,14\}$ and $\mathcal{Q}=\{3,4,7,8,11,12,15,16\}$ represent the sets of points where the first bit of the second STA is zero and one, respectively (refer to C_p and C_q in Fig. 2(b)). Also, $\delta_{p,q}$ is equal to (5) where $\alpha_{p,q}$, $\beta_{p,q}$, and $\zeta_{p,q}$ are given in Table 2 for all p ($\in\mathcal{P}$) and q ($\in\mathcal{Q}$). The expectation term is the same as (8).

C. DIVERSITY ORDER

From the analytical BER expression in (7) and (9), by using the Taylor series expansion under the high SNR regime, i.e., $\rho_n\to\infty$, the BER upper bound can be approximated as

$$P_{b,n}\approx\frac{10}{\sigma_n^2}\sum_{v=1}^{V}\frac{a_v}{b_v^2}\frac{1}{\rho_n^2}.\tag{10}$$

We can intuitively observe that the approximated expression is independent of $\zeta_{p,q}$. In other words, the BER performance of the uplink CR-STLC NOMA system is not related to the inter-rotation angle in the high SNR regime.

The diversity order of each STA, denoted by η_n, can be derived as follows:

$$\eta_n\triangleq-\lim_{\rho_n\to\infty}\frac{\log P_{b,n}}{\log\rho_n}\approx-\lim_{\rho_n\to\infty}\frac{\log\left(\frac{10}{\sigma_n^2}\sum_{v=1}^{V}\frac{a_v}{b_v^2}\rho_n^{-2}\right)}{\log\rho_n}=2.\tag{11}$$

From (11), it is clear that the uplink CR-STLC NOMA achieves the optimal spatial diversity order of two for both STAs when there are two STAs, which is the same as the OMA with two receive antennas in the AP.

D. DIVERSITY ORDER FOR MORE THAN TWO STAS

From now on, we consider an uplink CR-STLC NOMA system with more than two STAs. Although we can straightforwardly obtain the mathematical BER expressions of the uplink CR-STLC NOMA system for N STAs by defining N sets of 4^{2N-1} Euclidean distances as the aforementioned approach, the complexity of the error rate calculation increases exponentially with the number of STAs [27]. From this perspective, we analyze the generalized spatial diversity order to present the BER behavior in the high SNR regime instead of the BER performance itself for N STAs.

For convenience and w.l.o.g., we only consider the QPSK symbols of STAs for the first time-slot, and define a set

$\mathcal{K} = \{n | x_{n,1} \neq \widehat{x}_{n,1}, \forall n\}$. We also define K as the number of elements in set $\mathcal{K}$, i.e., $K = |\mathcal{K}|$, and w.l.o.g. assume that $x_{n,1} \neq \widehat{x}_{n,1}$ for $1 \leq n \leq K$ and $x_{n,1} = \widehat{x}_{n,1}$ for $K < n \leq N$. Note that we have proved from (11) that the uplink CR-STLC NOMA system achieves the optimal diversity order of two when $K = 2$. Let $\mathbf{x}_i = [x_{1,1}^{(i)}, \ldots, x_{N,1}^{(i)}]$ ($i \in \{1, 2, \ldots, 4^N\}$) be a vector consisting of the QPSK symbols of N STAs for representing constellation points, where $x_{n,1}^{(i)} = c_{((\lfloor (i-1)/4^{n-1} \rfloor \bmod 4)+1)}$. For example, if $N = 4$ and $i = 200$, then $\mathbf{x}_{200} = [c_4, c_2, c_1, c_4]$. We then define the general constellation point of superimposed QPSK symbols from N STAs in the uplink CR-STLC NOMA system as $C(\mathbf{x}_i) = \sum_{n=1}^{N} \sqrt{P_n \gamma_n} x_{n,1}^{(i)} e^{j\theta_n}$. Also, we assume that all STAs have the same transmit power, i.e., $P_n = P$, $\forall n$.

Given the channel gains, an upper bound on the conditional pairwise error probability (PEP) for $i \neq j$ can be derived as follows:

$$\begin{aligned}
&\Pr(\mathbf{x}_i \to \mathbf{x}_j | \gamma_1, \ldots, \gamma_N, \theta_1, \ldots, \theta_N) \\
&= \Pr\big(\Re[W] > |C(\mathbf{x}_i) - C(\mathbf{x}_j)|/2\big) \\
&\leq \Pr\big(W > |C(\mathbf{x}_i) - C(\mathbf{x}_j)|/2\big) \\
&= \Pr\left(W > \left| \sum_{n=1}^{K} \sqrt{P\gamma_n} \widetilde{x}_n^{(i,j)} e^{j\theta_n} \right| \Big/ 2 \right) \\
&\overset{(b)}{=} \exp\left(- \left| \sum_{n=1}^{K} \sqrt{P\gamma_n} \widetilde{x}_n^{(i,j)} e^{j\theta_n} \right|^2 \Big/ 8N_0 \right), \qquad (12)
\end{aligned}$$

where $\widetilde{x}_n^{(i,j)} \triangleq x_{n,1}^{(i)} - x_{n,1}^{(j)}$ and a random variable is defined as $W := |w_{1,1} + w_{2,2}^*|$ for noise in (3). Since the PDF of W is given by $f_W(w) = (w/N_0)\exp(-w^2/2N_0)$, (b) is satisfied.

From the following derivation, it does not depend on the specific constellation points, so we denote $\widetilde{x}_n^{(i,j)}$ as $\widetilde{x}_n$ for the convenience of notation. Assuming that $\widetilde{x}_1 e^{j\theta_1} \perp \widetilde{x}_2 e^{j\theta_2}$, w.l.o.g., $\widetilde{x}_1 e^{j\theta_1} \in \mathbb{R}$ and $j\widetilde{x}_2 e^{j\theta_2} \in \mathbb{R}$, and (12) can then be stated as follows[3]:

$$\begin{aligned}
&\exp\left(-\frac{1}{8} \left| \sum_{n=1}^{K} \sqrt{\rho\gamma_n} \widetilde{x}_n e^{j\theta_n} \right|^2 \right) \\
&= \exp\left(-\frac{1}{8} \left| \sqrt{\rho\gamma_1} \widetilde{x}_1 + \sum_{n=3}^{K} \Re\Big[\sqrt{\rho\gamma_n} \widetilde{x}_n e^{j\theta_n} \Big] \right. \right. \\
&\quad \left. \left. + j \left(\sqrt{\rho\gamma_2} \widetilde{x}_2 + \sum_{n=3}^{K} \Im\Big[\sqrt{\rho\gamma_n} \widetilde{x}_n e^{j\theta_n} \Big] \right) \right|^2 \right) \\
&= \exp\left(-\frac{\rho\big(\sqrt{\gamma_1}\widetilde{x}_1 + G_1\big)^2}{8} \right) \exp\left(-\frac{\rho\big(\sqrt{\gamma_2}\widetilde{x}_2 + G_2\big)^2}{8} \right), \qquad (13)
\end{aligned}$$

where $\rho = P/N_0$ and

$$G_1 = \sum_{n=3}^{K} \Re\Big[\sqrt{\gamma_n} \widetilde{x}_n e^{j\theta_n} \Big], \quad G_2 = \sum_{n=3}^{K} \Im\Big[\sqrt{\gamma_n} \widetilde{x}_n e^{j\theta_n} \Big].$$

Let (13) be a function denoted by $D(\mathbf{x}_i, \mathbf{x}_j)$ for simplicity. If $G_1 \geq 0$, then $D(\mathbf{x}_i, \mathbf{x}_j) \leq \exp(-\rho(\sqrt{\gamma_1}\widetilde{x}_1)^2/8) \cdot \exp(0)$, and by using the Taylor series expansion under the high SNR regime, we can derive

$$\begin{aligned}
&\mathbb{E}_{Z_1}\Big[\exp(-\rho(\sqrt{\gamma_1}\widetilde{x}_1)^2/8) \cdot \exp(0) \Big] \\
&= \int_0^{\infty} \exp\Big(-\rho(\sqrt{z_1}\widetilde{x}_1)^2/8 \Big) f_{Z_1}(z_1) dz_1 \approx \frac{64}{\sigma_1^2 \widetilde{x}_1^4} \rho^{-2}.
\end{aligned}$$

Based on the same approach as (11), this proves that the spatial diversity order is two. The same result is also given when $G_2 \geq 0$, so we can state that the diversity order of the PEP, $\Pr(\mathbf{x}_i \to \mathbf{x}_j)$, is greater than or equal to two (exactly two due to the degrees of freedom) when $G_1 \geq 0$ or $G_2 \geq 0$.

Now, we assume $G_1 > 0$, $G_2 > 0$ and define $D'(\mathbf{x}_i, \mathbf{x}_j) := \exp(-\rho(\sqrt{\gamma_1}\widetilde{x}_1 - G_1)^2/8) \cdot \exp(-\rho(\sqrt{\gamma_2}\widetilde{x}_2 - G_2)^2/8)$ to consider the opposite case. From (14) at the bottom of this page, w.l.o.g., we can derive

$$\begin{aligned}
&\mathbb{E}_{Z_1}\Big[\exp\Big(-\rho(\sqrt{z_1}\widetilde{x}_1 - G_1)^2/8 \Big) \Big] \\
&\leq \frac{\sqrt{32\pi}(G_1^2 \sigma_1 \widetilde{x}_1^2)^{3/2}}{(\sigma_1 \widetilde{x}_1^2 + 8/\rho)^{7/2}} \rho^{-1/2} + O(\rho^{-1}),
\end{aligned}$$

for a sufficiently high SNR. The PEP then can be derived as (15) at the bottom of the next page. Here, the remaining integrals with respect to z_n for $n \geq 3$ do not affect the exponent of ρ^{-1}. Therefore, (15) can be approximated as $F\rho^{-1} + O(\rho^{-3/2})$ in the high SNR regime for some constant F. This means that the diversity order of the PEP, $\Pr(\mathbf{x}_i \to \mathbf{x}_j)$, is greater than or equal to one for all N (≥ 3) STAs.

Let $C(\mathbf{x}_i^*)$ be the closest constellation point to $C(\mathbf{x}_i)$ among $C(\mathbf{x}_j)$ ($j \in \{1, 2, \ldots, 4^N\} \backslash i$) and δ_i^* be the Euclidean distance between the constellation points $C(\mathbf{x}_i)$ and $C(\mathbf{x}_i^*)$, i.e.,

3. We present Lemma 1 in APPENDIX A, which reveals that this assumption is sufficient to prove the statement.

$$\begin{aligned}
&\mathbb{E}_{Z_1}\Big[\exp\Big(-\rho\big(\sqrt{z_1}\widetilde{x}_1 - G_1\big)^2/8 \Big) \Big] = \int_0^{\infty} \exp\Big(-\rho(\sqrt{z_1}\widetilde{x}_1 - G_1)^2/8 \Big) f_{Z_1}(z_1) dz_1 \\
&= \frac{\sqrt{8\pi G_1^2 \sigma_1 \widetilde{x}_1^2}\big(G_1^2 \sigma_1 \widetilde{x}_1^2 \rho^3 + 12\sigma_1 \widetilde{x}_1^2 \rho^2 + 96\rho\big)}{\big(\sigma_1 \widetilde{x}_1^2 \rho + 8\big)^3 \sqrt{\sigma_1 \widetilde{x}_1^2 \rho + 8}} \left[\operatorname{erf}\left(\sqrt{\frac{1}{8}} \sqrt{\frac{G_1^2 \sigma_1 \widetilde{x}^2 \rho^2}{\sigma_1 \widetilde{x}^2 \rho + 8}} \right) + 1 \right] \exp\left(-\frac{G_1^2 \rho}{\sigma_1 \widetilde{x}_1^2 \rho + 8} \right) \\
&\quad + \frac{8\big(G_1^2 \sigma_1 \widetilde{x}_1^2 \rho^2 + 8\sigma_1 \widetilde{x}_1^2 \rho + 64\big)}{\big(\sigma_1 \widetilde{x}_1^2 \rho + 8\big)^3} \exp\left(-\frac{G_1^2 \rho}{8} \right) \qquad (14)
\end{aligned}$$

$\delta_i^* = \min_{j\in\{1,\ldots,4^N\}\setminus i} |C(\mathbf{x}_i) - C(\mathbf{x}_j)|$. Using a simple inequality, $\Pr(W > \delta) \le 4\Pr(\Re[W] > \delta/\sqrt{2})$, a lower bound of the conditional PEP can be derived as follows:

$$\begin{aligned}&\Pr\big(\mathbf{x}_i \to \mathbf{x}_i^* | \gamma_1, \ldots, \gamma_N, \theta_1, \ldots, \theta_N\big)\\ &\quad = \Pr\big(\Re[W] > \delta_i^*/2\big) \ge \frac{1}{4}\Pr\Big(W > \delta_i^*/\sqrt{2}\Big). \end{aligned} \tag{16}$$

Since the diversity order of the last inequality term is one according to the same derivation as above ((12) to (15)), we can state that the diversity order of $\Pr(\mathbf{x}_i \to \mathbf{x}_i^*)$ is less than or equal to one.

Using the Sandwich theorem, we can obtain

$$\frac{1}{4^N}\sum_{i=1}^{4^N}\Pr\big(\mathbf{x}_i \to \mathbf{x}_i^*\big) \le P_{b,n} \le \frac{1}{4^N}\sum_{i=1}^{4^N}\sum_{\substack{j=1\\ j\neq i}}^{4^N}\Pr\big(\mathbf{x}_i \to \mathbf{x}_j\big).$$

Here, the diversity order of the first inequality term is less than or equal to one, and the last inequality term is greater than or equal to one, i.e.,

$$\begin{aligned}1 \ge -\lim_{\rho\to\infty}\frac{\log\frac{1}{4^N}\sum_{i=1}^{4^N}\Pr\big(\mathbf{x}_i \to \mathbf{x}_i^*\big)}{\log\rho}\\ \ge \eta_n \ge -\lim_{\rho\to\infty}\frac{\log\frac{1}{4^N}\sum_{i=1}^{4^N}\sum_{\substack{j=1\\ j\neq i}}^{4^N}\Pr\big(\mathbf{x}_i \to \mathbf{x}_j\big)}{\log\rho} \ge 1.\end{aligned}$$

Hence, $1 \ge \eta_n \ge 1$, we can conclude that the uplink CR-STLC NOMA system for more than two STAs achieves the spatial diversity order of one.

IV. OPTIMIZING ROTATION ANGLE OF CR-STLC NOMA

Although it has been observed that the BER performance of the *two-user* uplink CR-STLC NOMA system is not closely related to the inter-rotation angle ($|\theta_1 - \theta_2|$) in the high SNR regime, performance optimization is required to achieve better BER in the practical SNR ranges. In this section, we introduce two methods to design the inter-rotation angle: dynamic rotation and fixed rotation.

A. DYNAMIC CONSTELLATION ROTATION METHOD

The rotation angle (w.l.o.g., $\theta_1 = 0$ and $\theta_2 = \theta$) can be instantaneously assigned according to the effective channel gain ratio of the two STAs to maximize $\delta_{\min}(\theta)$ which is the minimum Euclidean distance between the superimposed QPSK constellation points with respect to θ [23]. Considering, w.l.o.g., only the case that $P_1\gamma_1 \ge P_2\gamma_2$, two minimum distances $D_1(\theta)$ and $D_2(\theta)$ along θ are obtained by $D_1(\theta) = \sqrt{2P_1\gamma_1 + 2P_2\gamma_2 - 4\sqrt{P_1P_2}\sqrt{\gamma_1\gamma_2}\cos\theta}$ and $D_2(\theta) = \sqrt{2P_1\gamma_1 + 4P_2\gamma_2 - 4\sqrt{P_1P_2}\sqrt{\gamma_1\gamma_2}\mu}$ from (5), respectively.[4] From these, $\delta_{\min}(\theta)$ can be defined as $\delta_{\min}(\theta) = \min(D_1(\theta), D_2(\theta))$, so θ^* can be obtained by solving the following:

$$\theta^* = \arg\max_{\theta}\min(D_1(\theta), D_2(\theta)), \ \text{for } 0^\circ < \theta < 45^\circ. \tag{17}$$

Here, since $D_1(\theta)$ is a monotonic increasing function and $D_2(\theta)$ is a monotonic decreasing function in the $\theta \in (0, 45)$, (17) can be solved from θ which satisfies $D_1(\theta^*) = D_2(\theta^*)$. In other words, the optimal rotation angle in terms of the minimum Euclidean distance is derived from the intersection point of $D_1(\theta)$ and $D_2(\theta)$. We can solve it, which gives:

$$\theta^* = \arcsin\left(\frac{1}{2}\sqrt{\frac{P_2\gamma_2}{P_1\gamma_1}}\right). \tag{18}$$

Finally, by also considering the case $P_1\gamma_1 < P_2\gamma_2$, it can be generalized as follows:

$$\theta^* = \arcsin\left(\frac{1}{2}\sqrt{\frac{\min(P_1\gamma_1, P_2\gamma_2)}{\max(P_1\gamma_1, P_2\gamma_2)}}\right). \tag{19}$$

B. FIXED CONSTELLATION ROTATION METHOD

Although the dynamic rotation method achieves optimal BER performance irrespective to the SNR value, it causes significant signaling overhead because each STA needs to continuously receive θ^* from the AP.

It is more practical to assign a fixed rotation angle that takes into account the expected effective channel gain ratio of the two STAs. Specifically, using the analytical BER expressions in (7) and (9), we can obtain θ^*_{avg} that minimizes the average BER. Let $P_{b,\mathsf{avg}}$ be the average BER of the two STAs in the two-user uplink CR-STLC NOMA system,

4. The opposite case, i.e., $P_1\gamma_1 < P_2\gamma_2$, can be derived similarly by defining $D_2(\theta) = \sqrt{4P_1\gamma_1 + 2P_2\gamma_2 - 4\sqrt{P_1P_2}\sqrt{\gamma_1\gamma_2}\mu}$.

$$\begin{aligned}&\Pr\big(\mathbf{x}_i \to \mathbf{x}_j\big) \le \mathbb{E}_{Z_n}\big[D'\big(\mathbf{x}_i, \mathbf{x}_j\big)\big]\\ &= \int\cdots\int_{\mathbb{R}_+^N} D'(\mathbf{x}_i, \mathbf{x}_j) f_{Z_1}\cdots f_{Z_N}(z_n)dz_1\cdots dz_N\\ &\le \int\cdots\int_{\mathbb{R}_+^{N-2}}\left[\frac{\sqrt{32\pi}\big(G_1^2\sigma_1\widetilde{x}_1^2\big)^{3/2}}{\big(\sigma_1\widetilde{x}_1^2 + 8/\rho\big)^{7/2}}\rho^{-\frac{1}{2}} + O\Big(\rho^{-1}\Big)\right]\left[\frac{\sqrt{32\pi}\big(G_2^2\sigma_2\widetilde{x}_2^2\big)^{3/2}}{\big(\sigma_2\widetilde{x}_2^2 + 8/\rho\big)^{7/2}}\rho^{-\frac{1}{2}} + O\Big(\rho^{-1}\Big)\right] f_{Z_3}(z_3)\cdots f_{Z_N}(z_N)dz_3\cdots dz_N\\ &= \int\cdots\int_{\mathbb{R}_+^{N-2}}\frac{32\pi\big(G_1^2\sigma_1\widetilde{x}_1^2\big)^{3/2}\big(G_2^2\sigma_2\widetilde{x}_2^2\big)^{3/2}}{\big(\sigma_1\widetilde{x}_1^2 + 8/\rho\big)^{7/2}\big(\sigma_2\widetilde{x}_2^2 + 8/\rho\big)^{7/2}}\rho^{-1} + O\Big(\rho^{-3/2}\Big) f_{Z_3}(z_3)\cdots f_{Z_N}(z_N)dz_3\cdots dz_N\end{aligned} \tag{15}$$

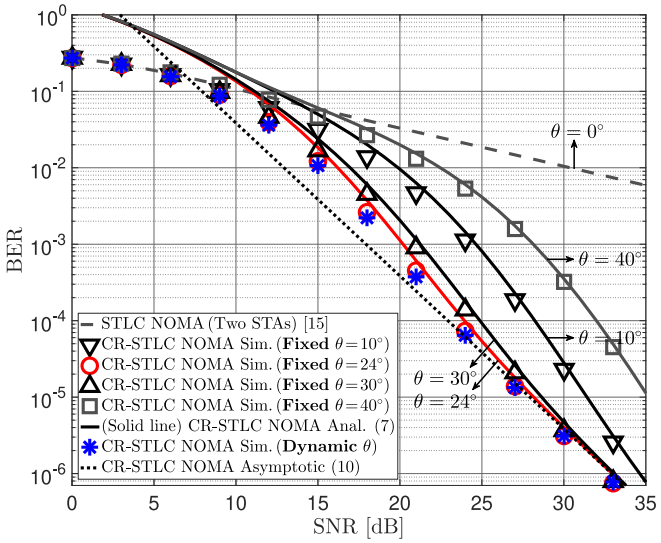

FIGURE 3. Average BER performance of two STAs for various constellation rotation angles in the two-user uplink CR-STLC NOMA system when $\mathbb{E}[P_1\gamma_1] = \mathbb{E}[P_2\gamma_2]$.

i.e., $P_{b,\text{avg}} \triangleq (P_{b,1} + P_{b,2})/2$. By exploiting critical point theorem, θ^*_{avg} can then be derived as follows:

$$\theta^*_{\text{avg}} = \left\{\theta \middle| \frac{dP_{b,\text{avg}}}{d\theta} = 0\right\}, \text{ for } 0^\circ < \theta < 45^\circ. \quad (20)$$

V. SIMULATION RESULTS

The BER performance of the uplink CR-STLC NOMA system and its mathematical analysis results in Section III are verified through Monte-Carlo simulations. First, the two-user uplink IoT network is considered to verify the BER performance analysis results of the CR-STLC NOMA performed in Section III, and then the simulation results considering more than two STAs or other modulation schemes are presented. From now on, we assume $P_n = P$, $\forall n$. That is, all STAs transmit their CR-STLC signals, (1), with the same average power.

Fig. 3 shows the BER performance of each STA versus the transmission SNR, $\rho = P/N_0$, in the two-user uplink CR-STLC NOMA system when $\mathbb{E}[\gamma_1] = \mathbb{E}[\gamma_2]$ ($\sigma_1 = \sigma_2 = 1$) and $V = 50$. Since $\mathbb{E}[P_1\gamma_1] = \mathbb{E}[P_2\gamma_2]$, it can also be represented as the average BER performance for both STAs. For the fixed constellation rotation method, we choose $\theta \in \{10, 24, 30, 40\}$ regardless of SNR values as examples. Recall in Section IV that we have introduced two constellation rotation angle design methods (*dynamic* or *fixed*) to achieve better BER performance in the mid and low SNR regimes. According to the SNR through numerical results based on (20), we obtain θ^*_{avg} as shown in Fig. 4, which is around 24°. We can observe from this figure that the two-user uplink CR-STLC NOMA system has various optimal rotation angles according to the transmit SNR and channel variance of each STA. Interestingly as shown in Fig. 3, a near-optimal BER performance becomes achieved over all SNR values if we set that $\theta = 24^\circ$ for the fixed constellation rotation method.

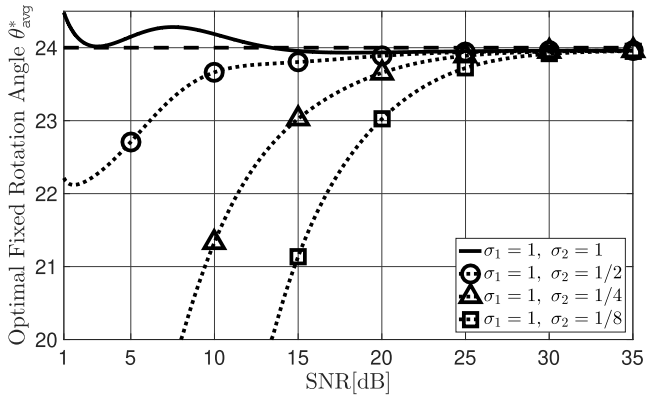

FIGURE 4. Optimal rotation angle of the fixed constellation rotation method for two STAs according to the SNR.

On the other hand, we can show in Fig. 3 that the average BER performance of the uplink CR-STLC NOMA ($\theta \neq 0$) is significantly improved over the STLC NOMA ($\theta = 0$) as well as the optimal diversity is achieved (11). Of course, the dynamic rotation method shows the best BER performance in the entire SNR regime. However, it can also be observed that the fixed rotation method is comparable to the dynamic rotation method with the significantly reduced signaling overhead because it does not require instantaneous rotation angle feedback. It is also observed that the BER upper bound analysis results are well matched to the Monte-Carlo simulations,[5] and that the average BER performance of the uplink CR-STLC NOMA in the high SNR regime is independent of the inter-rotation angle as discussed in Section III.

Fig. 5 compares the performance of the uplink CR-STLC NOMA with both the conventional two-user uplink NOMA technique and the OMA-based two-user STLC. To the best of our knowledge, there is no uplink NOMA system considering CSIT except for our previous studies [15], [16]. CSIR was assumed in conventional NOMA systems in the literature. From Fig. 5, we observe that the constellation rotation method slightly improves the BER performance in the uplink NOMA system with CSIR. In contrast, the constellation rotation method significantly improves the BER in the uplink CR-STLC NOMA system. Although the uplink CR-STLC NOMA results in worse BER performance than [23], the signaling overhead due to CSI sharing and rotation angle acquisition is significantly lower than [23] because only transmitters (STAs) need to know full CSI and each STA adopts a fixed rotation angle.

Furthermore, the BER performance of the two-user uplink CR-STLC NOMA approaches that of the OMA-based STLC system as the SNR increases.[6] It is meaningful that even

5. Due to the basic property of union bound, the analytical expressions are not tight in the low SNR regime. Specifically, the union bound of the BER is derived by summing the exclusive PEPs even though there exist many intersection regions in the probability space for the low SNR regime [26].

6. we analytically proved in APPENDIX B that the BER performances of the two systems are exactly the same in the high SNR region.

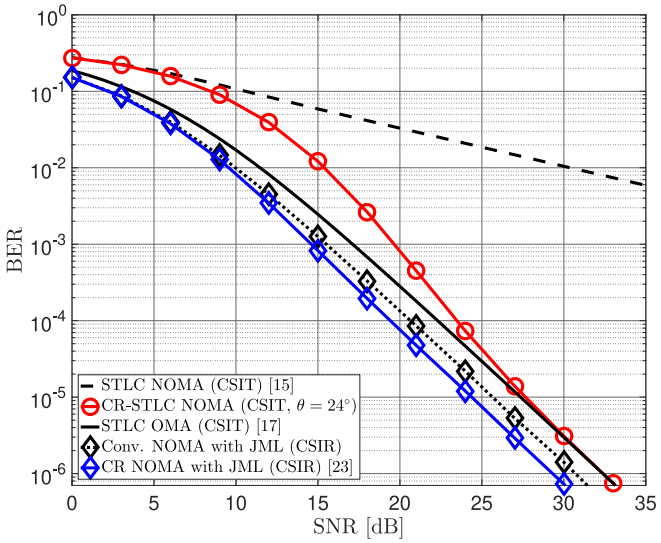

FIGURE 5. Average BER performance of two STAs in the two-user uplink CR-STLC NOMA, STLC NOMA, STLC OMA, and CSIR NOMA systems.

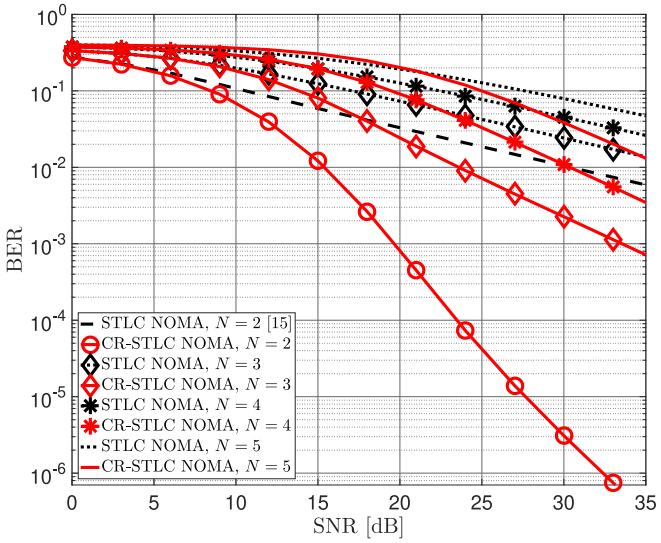

FIGURE 6. Average BER performance of *N* STAs with QPSK modulation in the uplink CR-STLC NOMA system.

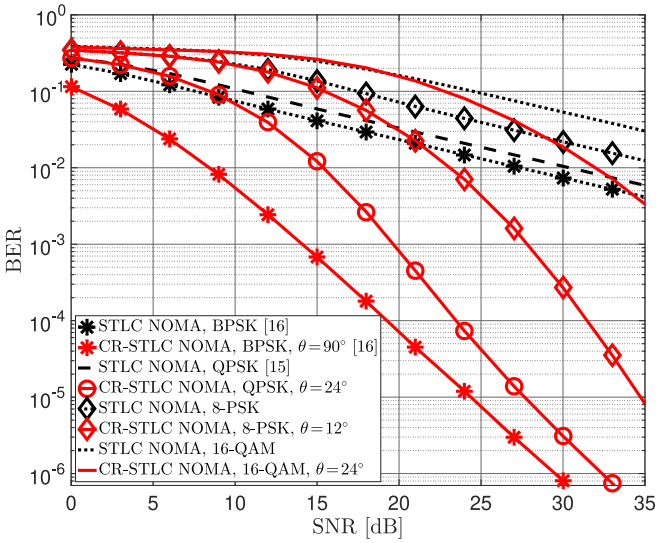

FIGURE 7. Average BER performance of two STAs in the two-user uplink CR-STLC NOMA system for different modulation schemes.

if two STAs simultaneously send their signals using the same radio resources, a quite similar performance with the OMA scheme is achieved as if there would be no inter-STA interference. Also, it should be emphasized that the proposed CR-STLC NOMA doubles the uplink throughput compared to the conventional OAM-based STLC while satisfying the error performance requirement.

Figs. 6 and 7 show the BER performance of the uplink CR-STLC NOMA system considering multiple STAs and M-ary modulations, respectively. Specifically, Fig. 6 shows the BER performance of the uplink CR-STLC NOMA system with N STAs when there exist more than two STAs with QPSK modulation and $\sigma_n = 1$, $\forall n$. The rotation angles are set to $\boldsymbol{\theta} = [0, 15, 30]$ for $N = 3$, $\boldsymbol{\theta} = [0, 12, 24, 36]$ for $N = 4$, and $\boldsymbol{\theta} = [0, 9, 18, 27, 36]$ for $N = 5$, respectively, where $\boldsymbol{\theta} = [\theta_1, \theta_2, \ldots, \theta_N]$. As discussed in Section III, the uplink CR-STLC NOMA system with two STAs achieves an optimal spatial diversity gain of 2, but the diversity order when there exist more than two STAs becomes 1. Somewhat interestingly, this is a very meaningful result in the sense that all STAs obtain the improved spatial diversity gain compared to that without constellation rotations.

Fig. 7 shows the BER performance of the uplink CR-STLC NOMA system with two STAs for various M-ary modulations. For the rotation angle, we set $\theta = 12°$ for 8-PSK and $\theta = 24°$ for 16-QAM modulations. It is worth noting that constellation rotation significantly improves the BER performance of the two-user uplink CR-STLC NOMA system as in the case of QPSK modulation. Based on the BER tendency in the high SNR regime shown in Fig. 7, we expect that the CR-STLC technique achieves the optimal spatial diversity gain regardless of the modulation schemes in the two-user uplink NOMA networks.

On the other hand, in practical IoT networks, there may exist estimation errors not only in the CSI at each STA but also in the effective channel gain at the AP. These estimation errors result from the time-varying nature of wireless channels or imperfection of channel estimation techniques in general. Such a channel uncertainty is modeled as $\widetilde{h}_{n,m} \triangleq h_{n,m} + \epsilon_{n,m}$, where $\widetilde{h}_{n,m}$ and $h_{n,m}$ denote the exact (or current) CSI and the estimated (or outdated) CSI, respectively, and $\epsilon_{n,m}$ represents the estimation error [17]. The resultant estimation error is assumed to follow i.i.d. complex Gaussian distribution with a zero mean and variance of σ_ϵ^2, where variance σ_ϵ^2 represents a mean-squared error (MSE) of estimation, i.e., $\mathbb{E}[|h_{n,m} - \widetilde{h}_{n,m}|] = \sigma_\epsilon^2$. Fig. 8 shows the average BER performance of two STAs in the two-user uplink CR-STLC NOMA system for varying the effect of channel estimation error when $\sigma_1 = \sigma_2 = 1$ and

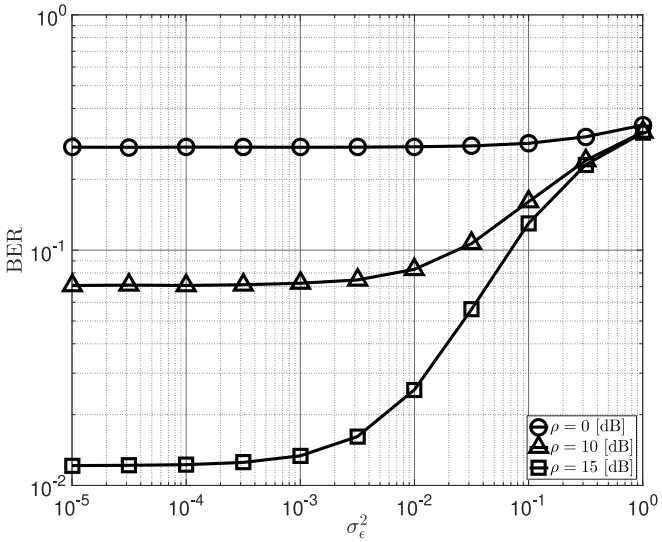

FIGURE 8. Average BER performance of two STAs in the two-user uplink CR-STLC NOMA system for channel estimation error.

$\theta = 24°$. As expected, the BER performance become gradually deteriorated as the CSI uncertainty σ_ϵ^2 increases, but it seems to be tolerant until $\sigma_\epsilon^2 = 10^{-3}$.

VI. CONCLUSION

We have investigated the uplink non-orthogonal multiple access (NOMA) system with a constellation-rotated space-time line code (CR-STLC). In particular, we have mathematically analyzed the BER upper bound of each IoT device (station: STA) in the two-user uplink CR-STLC NOMA system and found that the optimal spatial diversity gain could be achieved regardless of the inter-constellation rotation angle of the two STAs. However, to achieve better BER performance in the mid and low SNR regime, we have applied the inter-rotation angle optimization methods named dynamic rotation and fixed rotation. We found that the fixed rotation method with an optimal rotation angle achieves almost the same performance as the dynamic rotation method and obtained that value as $\theta^*_{\mathsf{avg}} \approx 24°$. Simulation results have verified our mathematical analyses. Finally, we show that the uplink CR-STLC NOMA system still achieves the spatial diversity order of 1 even if more than two IoT devices send packets to an access point (AP) simultaneously. Although it is not the optimal diversity order, the proposed system is still meaningful in the sense that all STAs obtain an improved spatial diversity gain compared to that without constellation rotation. As a further study on the uplink CR-STLC NOMA system, we will analyze the generalized BER performance for more than two STAs and arbitrary modulation schemes.

APPENDIX A

Lemma 1: It is sufficient to prove the spatial diversity order of the multi-user uplink CR-STLC NOMA system with assumption $\widetilde{x}_1 e^{j\theta_1} \perp \widetilde{x}_2 e^{j\theta_2}$.

Proof: Let ϕ $(\in (0, \pi))$ be the angle difference between $\widetilde{x}_1 e^{j\theta_1}$ and $\widetilde{x}_2 e^{j\theta_2}$. Then, w.l.o.g., we can denote that $\widetilde{x}_1 e^{j\theta_1} \in \mathbb{R}$ and $e^{-j\phi}\widetilde{x}_2 e^{j\theta_2} \in \mathbb{R}$. Using $\widetilde{x}_n e^{j\theta_n} = a_n + b_n e^{j\phi}$ and

$$\begin{aligned}|a_n + b_n e^{j\phi}|^2 &= a_n^2 + b_n^2 + 2a_n b_n \cos\phi \\ &\geq \min(1, 1+\cos\phi)\left(a_n^2 + b_n^2\right),\end{aligned}$$

where $a_n = \Re[\widetilde{x}_n e^{j\theta_n}] - \Im[\widetilde{x}_n e^{j\theta_n}]\cot\phi$ and $b_n = \frac{\Im[\widetilde{x}_n e^{j\theta_n}]}{\sin\phi}$, (12) can be stated as (21) at the bottom of the page. Since coefficients do not affect the spatial diversity order, we can state that the assumption is sufficient. ■

APPENDIX B

When all STAs use orthogonal radio resource blocks in an uplink IoT network, each STA can send signals without interference from other STAs. Hence, this can be equivalently regarded as a single-user STLC system for each resource block, and from [17, eq. (16)] the BER performance of the STA n, $P_{b,n}^{(\mathsf{OMA})}$, can be approximated for the high SNR regime as follows:

$$\begin{aligned}P_{b,n}^{(\mathsf{OMA})} &\leq \mathbb{E}_{Z_n}\left[Q\left(\sqrt{\frac{\rho_n\gamma_n}{2}}\right) + Q\left(\sqrt{\rho_n\gamma_n}\right)\right] \\ &\leq \frac{1}{2}\mathbb{E}_{Z_n}\left[\sum_{v=1}^{V} a_v\left\{\exp\left(-b_v\frac{\rho_n\gamma_n}{4}\right) + \exp\left(-b_v\frac{\rho_n\gamma_n}{2}\right)\right\}\right] \\ &= \sum_{v=1}^{V} a_v\left(\frac{8}{(b_v\rho_n\sigma_n)^2} + \frac{2}{(b_v\rho_n\sigma_n)^2}\right) \approx \frac{10}{\sigma_n^2}\sum_{v=1}^{V}\frac{a_v}{b_v}\frac{1}{\rho_n^2}.\end{aligned} \tag{22}$$

Although it can be tractably derived without an upper-bound of the Q-function, the exponential bound is exploited for a

$$\begin{aligned}&\exp\left(-\frac{1}{8}\left|\sum_{n=1}^{K}\sqrt{\rho\gamma_n}\widetilde{x}_n e^{j\theta_n}\right|^2\right) \\ &= \exp\left(-\frac{1}{8}\left|\sqrt{\rho\gamma_1}\widetilde{x}_1 + \sum_{n=3}^{K}\left(\Re\left[\sqrt{\rho\gamma_n}\widetilde{x}_n e^{j\theta_n}\right] - \Im\left[\sqrt{\rho\gamma_n}\widetilde{x}_n e^{j\theta_n}\right]\cot\phi\right) + e^{j\phi}\left(\sqrt{\rho\gamma_2}\widetilde{x}_2 + \sum_{n=3}^{K}\frac{\Im\left[\sqrt{\rho\gamma_n}\widetilde{x}_n e^{j\theta_n}\right]}{\sin\phi}\right)\right|^2\right) \\ &\leq \exp\left(-\frac{\rho\min(1, 1+\cos\phi)\left(\sqrt{\gamma_1}\widetilde{x}_1 + G_1'\right)^2}{8}\right)\exp\left(-\frac{\rho\min(1, 1+\cos\phi)\left(\sqrt{\gamma_2}\widetilde{x}_2 + G_2'\right)^2}{8}\right)\end{aligned} \tag{21}$$

fair comparison with (10). By comparing (22) with (10), we observe that the CR-STLC NOMA achieves the same BER performance as the OMA-based STLC in the high SNR regime in the two-user uplink IoT network.

ACKNOWLEDGMENT

The authors would like to thank Jaewon Bae for his invaluable assistance in analyzing the spatial diversity order of the CR-STLC NOMA system for more than two STAs in Section III-D.

REFERENCES

[1] Z. Zhang *et al.*, "6G wireless networks: Vision, requirements, architecture, and key technologies," *IEEE Veh. Technol. Mag.*, vol. 14, no. 3, pp. 28–41, Sep. 2019.

[2] F. Tariq, M. R. A. Khandaker, K.-K. Wong, M. A. Imran, M. Bennis, and M. Debbah, "A speculative study on 6G," *IEEE Wireless Commun.*, vol. 27, no. 4, pp. 118–125, Aug. 2020.

[3] M. Shirvanimoghaddam, M. Dohler, and S. J. Johnson, "Massive non-orthogonal multiple access for cellular IoT: Potentials and limitations," *IEEE Commun. Mag.*, vol. 55, no. 9, pp. 55–61, Sep. 2017.

[4] S. K. Sharma and X. Wang, "Toward massive machine type communications in ultra-dense cellular IoT networks: Current issues and machine learning-assisted solutions," *IEEE Commun. Surveys Tuts.*, vol. 22, no. 1, pp. 426–471, 1st Quart., 2020.

[5] X. Chen, N. Al-Dhahir, E. G. Larsson, W. Yu, D. W. K. Ng, and R. Schober, "Massive access for 5G and beyond," *IEEE J. Sel. Areas Commun.*, vol. 39, no. 3, pp. 615–637, Mar. 2021.

[6] K. Yang, N. Yang, N. Ye, M. Jia, Z. Gao, and R. Fan, "Non–orthogonal multiple access: Achieving sustainable future radio access," *IEEE Commun. Mag.*, vol. 57, no. 2, pp. 116–121, Feb. 2019.

[7] Z. Wei, L. Yang, D. W. K. Ng, J. Yuan, and L. Hanzo, "On the performance gain of NOMA over OMA in uplink communication systems," *IEEE Trans. Commun.*, vol. 68, no. 1, pp. 536–568, Jan. 2020.

[8] M. B. Shahab, S. J. Johnson, M. Shirvanimoghaddam, M. Chafii, E. Basar, and M. Dohler, "Index modulation aided uplink NOMA for massive machine type communications," *IEEE Wireless Commun. Lett.*, vol. 9, no. 12, pp. 2159–2162, Dec. 2020.

[9] M. B. Shahab, S. J. Johnson, M. Shirvanimoghaddam, and M. Dohler, "Receiver design for uplink power domain NOMA with discontinuous transmissions," *IEEE Commun. Lett.*, vol. 25, no. 8, pp. 2738–2742, Aug. 2021.

[10] J. Gao, W. Zhuang, M. Li, X. Shen, and X. Li, "MAC for machine type communications in industrial IoT—Part I: Protocol design and analysis," *IEEE Internet Things J.*, vol. 8, no. 12, pp. 9945–9957, Jun. 2021.

[11] J. Choi and J. Seo, "Evolutionary game for hybrid uplink NOMA with truncated channel inversion power control," *IEEE Trans. Commun.*, vol. 67, no. 12, pp. 8655–8665, Dec. 2019.

[12] X. Jiang and F. Kaltenberger, "Channel reciprocity calibration in TDD hybrid beamforming massive MIMO systems," *IEEE J. Sel. Topics Signal Process.*, vol. 12, no. 3, pp. 422–431, Jun. 2018.

[13] E. Dahlman, S. Parkvall, and J. Sköld, *5G NR: The Next Generation Wireless Access Technology*. New York, NY, USA: Academic, 2018.

[14] "6G: The next hyper—Connected experience for all," Samsung, Suwon, South Korea, White Paper, Dec. 2020. [Online]. Available: https://cdn.codeground.org/nsr/downloads/researchareas/20201201_6G_Vision_web.pdf

[15] K.-H. Lee, J. S. Yeom, B. C. Jung, and J. Joung, "A novel non–orthogonal multiple access with space–time line codes for massive IoT networks," in *Proc. IEEE 90th Veh. Technol. Conf. (VTC-Fall)*, Honolulu, HI, USA, Sep. 2019, pp. 1–5.

[16] J. Bae, K.-H. Lee, J. M. Kim, B. C. Jung, and J. Joung, "Performance analysis of uplink NOMA-IoT networks with space-time line code," in *Proc. IEEE 90th Veh. Technol. Conf. (VTC-Fall)*, Honolulu, HI, USA, Sep. 2019, pp. 1–5.

[17] J. Joung, "Space–time line code," *IEEE Access*, vol. 6, pp. 1023–1041, 2018.

[18] J. Joung and B. C. Jung, "Machine learning based blind decoding for space–time line code (STLC) systems," *IEEE Trans. Veh. Technol.*, vol. 68, no. 5, pp. 5154–5158, May 2019.

[19] S.-C. Lim and J. Joung, "Transmit antenna selection for space–time line code systems," *IEEE Trans. Commun.*, vol. 69, no. 2, pp. 786–798, Feb. 2021.

[20] J. Choi and J. Joung, "Generalized space–time line code with receive combining for MIMO systems," *IEEE Syst. J.*, early access, Mar. 18, 2021, doi: 10.1109/JSYST.2021.3060134.

[21] M. Qiu, Y.-C. Huang, and J. Yuan, "Downlink non-orthogonal multiple access without SIC for block fading channels: An algebraic rotation approach," *IEEE Trans. Wireless Commun.*, vol. 18, no. 8, pp. 3903–3918, Aug. 2019.

[22] Y. Chang and K. Fukawa, "Phase rotated non–orthogonal multiple access for 3-user superposition signals," in *Proc. IEEE 90th Veh. Technol. Conf. (VTC-Fall)*, Honolulu, HI, USA, Sep. 2019, pp. 1–5.

[23] B. K. Ng and C. Lam, "Joint power and modulation optimization in two-user non-orthogonal multiple access channels: A minimum error probability approach," *IEEE Trans. Veh. Technol.*, vol. 67, no. 11, pp. 10693–10703, Nov. 2018.

[24] C.-H. Lin, S.-L. Shieh, T.-C. Chi, and P.-N. Chen, "Optimal inter-constellation rotation based on minimum distance criterion for uplink NOMA," *IEEE Trans. Veh. Technol.*, vol. 68, no. 1, pp. 525–539, Jan. 2019.

[25] N. Ye, A. Wang, X. Li, W. Liu, X. Hou, and H. Yu, "On constellation rotation of NOMA with SIC receiver," *IEEE Commun. Lett.*, vol. 22, no. 3, pp. 514–517, Mar. 2018.

[26] J. S. Yeom, H. S. Jang, K. S. Ko, and B. C. Jung, "BER performance of uplink NOMA with joint maximum–likelihood detector," *IEEE Trans. Veh. Technol.*, vol. 68, no. 10, pp. 10295–10300, Oct. 2019.

[27] C. Liu and N. C. Beaulieu, "Exact SER and BER analysis on jointly optimal maximum likelihood detection of two QPSK signals with phase offset," *IEEE Trans. Veh. Technol.*, vol. 70, no. 11, pp. 11695–11709, Nov. 2021.

[28] H. Semira, F. Kara, H. Kaya, and H. Yanikomeroglu, "Multi-user joint maximum-likelihood detection in uplink NOMA-IoT networks: Removing the error floor," *IEEE Wireless Commun. Lett.*, vol. 10, no. 11, pp. 2459–2463, Nov. 2021.

[29] H. Yahya, E. Alsusa, and A. Al-Dweik, "Exact BER analysis of NOMA with arbitrary number of users and modulation orders," *IEEE Trans. Commun.*, vol. 69, no. 9, pp. 6330–6344, Sep. 2021.

[30] W. Han, X. Ma, D. Tang, and N. Zhao, "Study of SER and BER in NOMA systems," *IEEE Trans. Veh. Technol.*, vol. 70, no. 4, pp. 3325–3340, Apr. 2021.

[31] Z. Xiang, W. Yang, Y. Cai, Z. Ding, Y. Song, and Y. Zou, "NOMA-assisted secure short-packet communications in IoT," *IEEE Wireless Commun.*, vol. 27, no. 4, pp. 8–15, Aug. 2020.

[32] D. J. C. MacKay, *Information Theory, Inference and Learning Algorithms*. New York, NY, USA: Cambridge Univ. Press, 2003.

[33] G. McLachlan and D. Peel, *Finite Mixture Models*. Hoboken, NJ, USA: Wiley, 2000.

[34] A. Salari, M. Shirvanimoghaddam, M. B. Shahab, R. Arablouei, and S. Johnson, "Clustering-based joint channel estimation and signal detection for grant-free NOMA," in *Proc. IEEE Globecom Workshops (GC Wkshps)*, Taipei, Taiwan, Dec. 2020, pp. 1–6.

[35] M. Chiani, D. Dardari, and M. K. Simon, "New exponential bounds and approximations for the computation of error probability in fading channels," *IEEE Trans. Wireless Commun.*, vol. 2, no. 4, pp. 840–845, Jul. 2003.

KI-HUN LEE (Student Member, IEEE) received the B.S. degree in electronics engineering from Chungnam National University, Daejeon, South Korea, in 2018, where he is currently pursuing the Ph.D. degree with the Department of Electronics Engineering.

His research interests include wireless communications, radio network planning and optimization, statistical signal processing, and machine learning.

JEONG SEON YEOM (Student Member, IEEE) received the B.S. and M.S. degrees in electronics engineering from Chungnam National University, Daejeon, South Korea, in 2017 and 2019, respectively, where he is currently pursuing the Ph.D. degree with the Department of Electronics Engineering.

His research interests include nonorthogonal multiple access, multiple-input multiple-output, and interference mitigation in wireless communication systems.

JINGON JOUNG (Senior Member, IEEE) received the B.S. degree in radio communication engineering from Yonsei University, Seoul, South Korea, in 2001, and the M.S. and Ph.D. degrees in electrical engineering and computer science from the Korea Advanced Institute for Science and Technology (KAIST), Daejeon, South Korea, in 2003 and 2007, respectively.

He was a Postdoctoral Fellow with KAIST and UCLA, Los Angeles, CA, USA, in 2007 and 2008, respectively. He was the Scientist of the Institute for Infocomm Research, Agency for Science, Technology and Research, Singapore, from 2009 to 2015, and joined Chung-Ang University (CAU), Seoul, in 2016, as a Faculty Member. He is currently an Associate Professor with the School of Electrical and Electronics Engineering, CAU, where he is also the Principal Investigator of the Intelligent Wireless Systems Laboratory. His research interests include wireless communication signal processing, numerical analysis, algorithms, and machine learning.

Dr. Joung was a recipient of the First Prize of the Intel-ITRC Student Paper Contest in 2006. He was recognized as the Exemplary Reviewers of IEEE COMMUNICATIONS LETTERS in 2012 and IEEE WIRELESS COMMUNICATIONS LETTERS in 2012, 2013, 2014, and 2019. He is an inventor of a Space–Time Line Code that is a fully symmetric scheme to a Space-Time Block Code, also known as Alamouti code. He has served as the Guest Editor for IEEE ACCESS in 2016, an Editorial Board Member for *APSIPA Transactions on Signal and Information Processing* from 2014 to 2019, a Guest Editor for the *Electronics* in 2019, and an Associate Editor for the *Sensors* in 2020. He has been currently serving as an Associate Editor for IEEE TRANSACTIONS ON VEHICULAR TECHNOLOGY since 2018.

BANG CHUL JUNG (Senior Member, IEEE) received the B.S. degree in electronics engineering from Ajou University, Suwon, South Korea, in 2002, and the M.S. and Ph.D. degrees in electrical and computer engineering from the Korea Advanced Institute for Science and Technology (KAIST), Daejeon, South Korea, in 2004 and 2008, respectively.

He was a Senior Researcher/Research Professor with the KAIST Institute for Information Technology Convergence, Daejeon, from 2009 to 2010. From 2010 to 2015, he was a Faculty Member of Gyeongsang National University, Tongyeong, South Korea. He is currently a Professor with the Department of Electronics Engineering, Chungnam National University, Daejeon. His research interests include wireless communication systems, Internet-of-Things communications, statistical signal processing, information theory, interference management, radio resource management, spectrum sharing techniques, and machine learning.

Dr. Jung was a recipient of the Fifth IEEE Communication Society Asia–Pacific Outstanding Young Researcher Award in 2011, the Bronze Prize of Intel Student Paper Contest in 2005, the First Prize of KAISTs Invention Idea Contest in 2008, and the Bronze Prize of Samsung Humantech Paper Contest in 2009. He has been selected as a winner of Haedong Young Scholar Award in 2015, which is sponsored by the Haedong foundation and given by KICS. He has been selected as a winner of the 29th Science and Technology Best Paper Award in 2019, which is sponsored by the Korean Federation of Science and Technology Societies. He has served as an Associate Editor of *IEEE Vehicular Technology Magazine* since 2020 and he has also served as an Associate Editor for the *IEICE Transactions on Fundamentals of Electronics, Communications, and Computer Sciences* since 2018.